Available online at www.sciencedirect.com

ScienceDirect

Mendeleev Commun., 2023, **33**, 337–339

Mendeleev Communications

Liposomes as nanoreactors for copper nanoparticles synthesis

Olga V. Zaborova,*[a] Sofia O. Livshitz,[a] Maria A. Kirsanova[b] and Vladimir G. Sergeyev[a]

[a] *Department of Chemistry, M. V. Lomonosov Moscow State University, 119991 Moscow, Russian Federation. E-mail: olga.zaborova@gmail.com*

[b] *Skolkovo Institute of Science and Technology, 121205 Moscow, Russian Federation*

DOI: 10.1016/j.mencom.2023.04.013

Copper nanoparticles 3.8–10.9 nm in size were synthesized in solid-phase membrane liposomes by a facile method of copper sulfate reduction with hydrazine. A change in the excess of hydrazine leads to the controlled formation of either Cu_2O or Cu^0 nanoparticles.

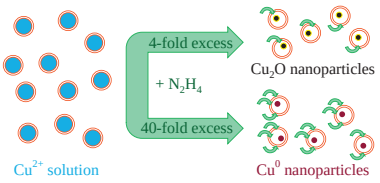

Keywords: copper nanoparticles, liposomal nanoreactors, transmission electron microscopy, nanoparticle tracking analysis.

Metal nanoparticles (MNPs) find their application in various fields due to their unique physicochemical properties. The large specific surface area makes it possible to use MNPs (Au, Ag, Cu, Pt, *etc.*) as catalysts.[1–3] Nanoparticles of metals with high conductivity and thermal stability (Ag, Au, Cu and Pd) are used for inkjet printing.[4,5] MNPs with surface plasmon resonance absorption are used in biomedical applications as diagnostic tools.[6,7] Moreover, nanoparticles of metals such as silver and copper have antibacterial, antifungal, anti-inflammatory and antiproliferative activities.[8] However, the use of MNPs *in vivo* is limited mainly due to their low colloidal stability. The use of various biocompatible stabilizers, such as proteins, hydrophilic polymers (polyvinylpyrrolidone, polyethylene glycol, polyethyleneimine),[10–13] organic polyacids (polyacrylic acid),[14] amphiphilic copolymers (Pluronic®),[15,16] amino acids,[17] carbohydrates[18] and surfactants,[19] can significantly increase the colloidal stability of MNPs. Another way to stabilize MNPs is to incorporate them into liposomes.[20]

Copper nanoparticles (CuNPs) are currently of great interest, since copper, having all the properties listed above, is cheaper than noble metals. However, CuNPs have one major drawback that limits their application, namely, rapid oxidation. Thus, in most cases, CuNPs are synthesized in an inert atmosphere[21,22] in the presence of stabilizers such as thiols, amines (including polyamines) and ascorbic acid, which should prevent both aggregation and oxidation of nanoparticles.[22–25] An interesting way for the synthesis of MNPs in the internal cavity of liposomes was previously reported elsewhere.[26–28] This strategy of using liposomes as nanoreactors makes it possible not only to control the rate of formation and, hence, the size and shape of MNPs, but also to stabilize the resulting nanoparticles with phospholipids. Reported studies describe the formation of gold, silver and platinum nanoparticles using relatively mild reducing agents such as sodium citrate, glycerol and ascorbic acid. In this article, we propose the synthesis of CuNPs in the internal cavity of liposomes loaded with a $CuSO_4$ solution using hydrazine as a reducing agent.

Liposomes containing a 1 M $CuSO_4$ solution in the internal cavity were prepared by extrusion[29] through a polycarbonate membrane with 50 nm pores. At the experimental temperature, the membrane of the obtained liposomes was in the solid phase state (see Online Supplementary Materials). Several studies[30] have reported the reduction of Cu^{2+} to Cu^0 with hydrazine, including reduction in reversed micelles.[31] Since it has been reported that the required excess of hydrazine is between 3 and 40 times, in the current study, we tested two systems with 4- and 40-fold excess.

The reduction of Cu^{2+} was monitored using UV-VIS spectroscopy. Figure 1(*a*) represents the change in the absorption spectra of liposomes after adding a 4-fold excess of hydrazine to liposomes loaded with $CuSO_4$. Immediately after the addition of hydrazine, two peaks appeared in the spectrum at 340 and 420 nm. The absorption peak at 340 nm (region I) is attributed to the formation of colloidal CuO particles,[32,33] and at 420 nm (region II) to Cu_2O.[32,34] The intensity of these two peaks increased within 20 min and then did not change. The color of the sample was light yellow. The addition of a 40-fold excess of hydrazine to the liposomes loaded with $CuSO_4$ [Figure 1(*b*)] resulted in an absorption peak at 580 nm (region III), which is a characteristic absorption peak for nanosized metallic copper.[22,35] After 10 min, a small peak appeared at 420 nm (region II), indicating the formation of Cu_2O nanoparticles. As the reaction proceeded, the intensity of the peak increased along with the increase in light scattering (an increase in the slope of the A *vs.* λ curve in the region of 700–900 nm). The color of the sample changed from dirty yellow to red.

Comparing the time-dependent absorption spectra of the two systems upon reduction of Cu^{2+} with a 4- and 40-fold excess of

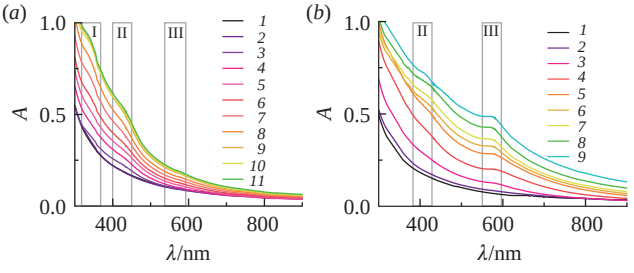

Figure 1 UV-VIS spectra during the formation of CuNPs in liposomes upon reduction with hydrazine, recorded (*a*) (*1*) before, (*2*) immediately and (*3*) 1, (*4*) 2, (*5*) 4, (*6*) 6, (*7*) 8, (*8*) 10, (*9*) 15, (*10*) 20 and (*11*) 30 min after adding a 4-fold excess of hydrazine and (*b*) (*1*) before, (*2*) immediately and (*3*) 2, (*4*) 5, (*5*) 10, (*6*) 15, (*7*) 20, (*8*) 30 and (9) 40 min after adding a 40-fold excess of hydrazine. Liposome concentration 0.72 mg cm^{-3}, T = 22 °C.

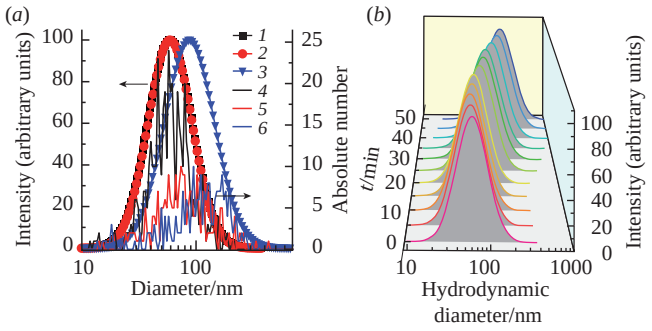

Figure 2 (*a*) Size distributions of liposomes loaded with $CuSO_4$ in terms of (*1*)–(*3*) intensity-weighted distribution measured by DLS and (*4*)–(*6*) absolute number distribution measured by NTA (*1*),(*4*) before, (*2*),(*5*) immediately and (*3*),(*6*) 30 min after adding the hydrazine solution. (*b*) Change in intensity-weighted liposome size distribution over time after addition of hydrazine. Liposome concentration 0.72 mg cm^{-3}, $[Cu^{2+}] / [N_2H_4] = 1:40$, $T = 22$ °C.

hydrazine in liposomes, we noted two differences. First, there are different absorption peaks, which seem to be associated with the formation of different reaction products. The addition of a 4-fold excess of hydrazine was accompanied by the formation of CuO and Cu_2O nanoparticles, while the addition of a 40-fold excess of hydrazine led to the predominant formation of Cu^0 nanoparticles. The addition of hydrazine to the liposomal suspension could not lead to an immediate reaction, since hydrazine must first penetrate the lipid membrane to reduce Cu^{2+}. The penetration of hydrazine into liposomes was additionally inhibited by the fact that the lipid membrane was in a solid phase state. Consequently, the reducing agent was dosed into the reaction and the portions were different in the two systems: at a 4-fold excess, the amount of hydrazine was only enough to reduce Cu^{2+} to Cu(I), and at a 40-fold excess, its amount was sufficient for complete reduction. Thus, we assume that the reduction process is divided into two steps, reduction to Cu(I) and subsequent reduction to Cu^0:

$$4\,CuSO_4 + 9\,N_2H_4 + 2\,H_2O \rightarrow 2\,Cu_2O\downarrow + N_2\uparrow + 4\,(N_2H_5)_2SO_4, \quad (1)$$

$$2\,Cu_2O + N_2H_4 \rightarrow 4\,Cu + N_2\uparrow + 2\,H_2O. \quad (2)$$

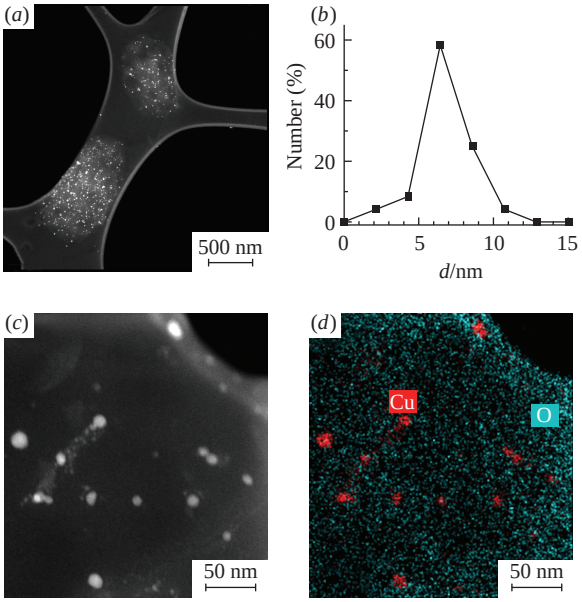

Figure 3 (*a*),(*c*) HAADF-STEM images of CuNPs in liposomes one day after hydrazine addition. (*b*) Statistical analysis of HAADF-STEM images of CuNPs in liposomes. (*d*) STEM-EDX mixed map of oxygen and copper corresponding to the image shown in (*c*). Liposome concentration 5 mg cm^{-3}, $[Cu^{2+}] / [N_2H_4] = 1:40$, $T = 22$ °C.

The second difference was the contribution of light scattering to the absorption spectra: at a 4-fold excess, it was negligibly small, while at a 40-fold excess, it was rather significant. This increase in light scattering could be attributed to the formation of large particles in the system. Since the reduction is accompanied by gas evolution and occurs in the internal cavity of the liposome, this can lead to rupture of the lipid membrane and fusion of liposomes. Therefore, using dynamic light scattering (DLS) and nanoparticle tracking analysis (NTA), we monitored the possible change in the size of liposomes for a system with a 40-fold excess of hydrazine. The mean diameter of the resulting liposomes was 58 nm with a PDI of 0.225 [Figure 2(*a*), curves *1* and *4*]. The size distributions obtained by the DLS and NTA methods are in good agreement.

The size distribution of liposomes was controlled immediately at the moment and 30 min after the addition of hydrazine [Figure 2(*a*), curves *2* and *3*]. The size of the liposomes increased significantly after 30 min. Moreover, the change in size distribution was already detectable by the NTA technique [Figure 2(*a*), curve *5*] immediately after the addition of hydrazine. As previously suggested, the gas evolution during the reaction can cause the disruption and fusion of liposomes. To follow this process, we performed DLS measurements every 5 min after the addition of hydrazine [Figure 2(*b*)]. One can see that during the first 20 min after the addition of hydrazine, the mean diameter and size distribution of liposomes did not change, while after that the size of liposomes began to increase.

The process of disruption of liposomes during the reaction was also indirectly detected on transmission electron micrographs. Figures 3(*a*),(*c*) represent HAADF-STEM images of CuNPs obtained one day after the addition of hydrazine, and only some traces of disrupted liposomes could be found in the sample. In addition, the images showed a huge amount of dense nanoparticles, which, as shown in the STEM-EDX map [Figure 3(*d*)], were Cu^0 nanoparticles.

We calculated the theoretical size of Cu^0 nanoparticles synthesized in liposomes, assuming that the mean liposome diameter is 60 nm [see Figure 2(*a*)] and the concentration of $CuSO_4$ inside the liposomes is 1 mol dm^{-3}. As a result of the calculation, the mean size of CuNPs was about 11.6 nm. Statistical analysis of HAADF-STEM images was performed using ImageJ software. The resulting CuNP size distribution is shown in Figure 3(*b*). The size of the obtained nanoparticles varied from 3.8 to 10.9 nm, which is in good agreement with the calculated values.

A new method for the synthesis of CuNP inside the internal cavity of liposomes with a membrane in the solid phase state has been developed. The formation of Cu^0 nanoparticles was confirmed by spectrophotometry (absorption peak at 580 nm) and STEM-EDX mapping. It has been shown that the reduction of copper salt inside the liposomes can be divided into two stages, including the preliminary formation of Cu_2O nanoparticles followed by reduction to Cu^0 nanoparticles. The possibility of controlling the depth of copper reduction by adding various amounts of hydrazine was shown for the first time, which leads to the formation of either Cu_2O or Cu^0 nanoparticles.

This work was supported by the Russian Science Foundation (project no. 21-73-20144). NTA experiments were carried out on the equipment of the MSU Shared Research Equipment Center ‘Technologies for obtaining new nanostructured materials and their complex study’, acquired by MSU in the framework of the Equipment Renovation Program (National project ‘Science’).

Online Supplementary Materials

Supplementary data associated with this article can be found in the online version at doi: 10.1016/j.mencom.2023.04.013.

References

1 D. T. Thompson, *Nano Today*, 2007, **2** (4), 40.
2 X.-Y. Dong, Z.-W. Gao, K.-F. Yang, W.-Q. Zhang and L.-W. Xu, *Catal. Sci. Technol.*, 2015, **5**, 2554.
3 T. S. Rodrigues, A. G. M. da Silva and P. H. C. Camargo, *J. Mater. Chem. A*, 2019, **7**, 5857.
4 N. C. Raut and K. Al-Shamery, *J. Mater. Chem. C*, 2018, **6**, 1618.
5 J. Cheon, J. Lee and J. Kim, *Thin Solid Films*, 2012, **520**, 2639.
6 W. Zhou, X. Gao, D. Liu and X. Chen, *Chem. Rev.*, 2015, **115**, 10575.
7 M. Larguinho and P. V. Baptista, *J. Proteomics*, 2012, **75**, 2811.
8 E. Sánchez-López, D. Gomes, G. Esteruelas, L. Bonilla, A. L. Lopez-Machado, R. Galindo, A. Cano, M. Espina, M. Ettcheto, A. Camins, A. M. Silva, A. Durazzo, A. Santini, M. L. Garcia and E. B. Souto, *Nanomaterials*, 2020, **10**, 292.
9 L. Guerrini, R. A. Alvarez-Puebla and N. Pazos-Perez, *Materials*, 2018, **11**, 1154.
10 M. Guzman, M. Arcos, J. Dille, S. Godet and C. Rousse, *Nano Biomed. Eng.*, 2018, **10**, 392.
11 K. M. Koczkur, S. Mourdikoudis, L. Polavarapu and S. E. Skrabalak, *Dalton Trans.*, 2015, **44**, 17883.
12 C. C. S. Batista, L. J. C. Albuquerque, I. de Araujo, B. L. Albuquerque, F. D. da Silva and F. C. Giacomelli, *RSC Adv.*, 2018, **8**, 10873.
13 Y. Wang, J. E. Q. Quinsaat, T. Ono, M. Maeki, M. Tokeshi, T. Isono, K. Tajima, T. Satoh, S. Sato, Y. Miura and T. Yamamoto, *Nat. Commun.*, 2020, **11**, 6089.
14 H. Jans, K. Jans, L. Lagae, G. Borghs, G. Maes and Q. Huo, *Nanotechnology*, 2010, **21**, 455702.
15 P. Alexandridis and M. Tsianou, *Eur. Polym. J.*, 2011, **47**, 569.
16 M. S. Holden, K. E. Nick, M. Hall, J. R. Milligan, Q. Chen and C. C. Perry, *RSC Adv.*, 2014, **4**, 52279.
17 L. Coronato Courrol and R. Almeida de Matos, in *Catalytic Application of Nano-Gold Catalysts*, ed. N. K. Mishra, InTech, Rijeka, Croatia, 2016, pp. 83–99.
18 Z. Shervani and Y. Yamamoto, *Carbohydr. Res.*, 2011, **346**, 651.
19 M. Guzman, M. Arcos, J. Dille, C. Rousse, S. Godet and L. Malet, *ACS Omega*, 2021, **6**, 18576.
20 M. Musielak, J. Potoczny, A. Boś-Liedke and M. Kozak, *Int. J. Mol. Sci.*, 2021, **22**, 6229.
21 C. Vázquez-Vázquez, M. Bañobre-López, A. Mitra, M. A. López-Quintela and J. Rivas, *Langmuir*, 2009, **25**, 8208.
22 B. Wang, S. Chen, J. Nie and X. Zhu, *RSC Adv.*, 2014, **4**, 27381.
23 G. D. M. R. Dabera, M. Walker, A. M. Sanchez, H. J. Pereira, R. Beanland and R. A. Hatton, *Nat. Commun.*, 2017, **8**, 1894.
24 N. Jardón-Maximino, M. Pérez-Alvarez, R. Sierra-Ávila, C. A. Ávila-Orta, E. Jiménez-Regalado, A. M. Bello, P. González-Morones and G. Cadenas-Pliego, *J. Nanomater.*, 2018, 9512768.
25 G. G. Jang, C. B. Jacobs, R. G. Gresback, I. N. Ivanov, H. M. Meyer, III, M. Kidder, P. C. Joshi, G. E. Jellison, Jr., T. J. Phelps, D. E. Graham and J.-W. Moon, *J. Mater. Chem. C*, 2015, **3**, 644.
26 G. Clergeaud, R. Genç, M. Ortiz and C. K. O'Sullivan, *Langmuir*, 2013, **29**, 15405.
27 S. Gudlur, C. Sandén, P. Matoušková, C. Fasciani and D. Aili, *J. Colloid Interface Sci.*, 2015, **456**, 206.
28 J.-H. Lee, Y. Shin, W. Lee, K. Whang, D. Kim, L. P. Lee, J.-W. Choi and T. Kang, *Sci. Adv.*, 2016, **2**, e1601838.
29 O. V. Zaborova, *Russ. J. Gen. Chem.*, 2020, **90**, 762.
30 S. V. Saikova, S. A. Vorob'ev, R. B. Nikolaeva and Yu. L. Mikhlin, *Russ. J. Gen. Chem.*, 2010, **80**, 1122 (*Zh. Obshch. Khim.*, 2010, **80**, 952).
31 C. Salzemann, I. Lisiecki, J. Urban and M.-P. Pileni, *Langmuir*, 2004, **20**, 11772.
32 Y. Zhao, J.-J. Zhu, J.-M. Hong, N. Bian and H.-Y. Chen, *Eur. J. Inorg. Chem.*, 2004, 4072.
33 M. Pérez-Alvarez, G. Cadenas-Pliego, O. Pérez-Camacho, V. E. Comparán-Padilla, C. J. Cabello-Alvarado and E. Saucedo-Salazar, *Polymers*, 2021, **13**, 1906.
34 M. Blosi, S. Albonetti, M. Dondi, C. Martelli and G. Baldi, *J. Nanopart. Res.*, 2011, **13**, 127.
35 G. G. Condorelli, L. L. Costanzo, I. L. Fragalà, S. Giuffrida and G. Ventimiglia, *J. Mater. Chem.*, 2003, **13**, 2409.

Received: 3rd November 2022; Com. 22/7038